

---

# Efficiency of controlled topical delivery of silver sulfadiazine in infected burn wounds

---

N. Shanmugasundaram, T. S. Uma, T. S. Ramyaa Lakshmi, Mary Babu

Biomaterials Division, Central Leather Research Institute - TICEL Biopark, Tharamani Road, Tharamani, Chennai 600 113, Tamil Nadu, India

Received 25 April 2007; revised 6 December 2007; accepted 30 January 2008

Published online 22 April 2008 in Wiley InterScience (www.interscience.wiley.com). DOI: 10.1002/jbm.a.31997

**Abstract:** The present study is designed to assess the potential benefits of controlled delivery of silver sulfadiazine from collagen scaffold (SSDM-CS) in infected deep partial thickness burn wounds in which epidermis is lost completely and the entire papillary dermis and most of the reticular layer of the dermis is lost. Infection induced by inoculating  $10^7$  colony forming units (cfu) of *Pseudomonas aeruginosa* caused significant increase in wound size (20%) till day 15, which decreased significantly from day 9 by SSDM-CS treatment, showing complete healing by day 27 (control  $\geq$  37 days). Early subsidence of infection ( $<10^2$  cfu, day 9) by SSDM-CS resulted in faster epidermal resurfacing and fibroplasia, whereas heavy microbial load ( $>10^7$  cfu, day 9) in controls caused severe inflammatory cellular infiltration. Persistent infection triggered early expression of proinflammatory cytokines interleukin-6, interleukin 1- $\beta$ ,

and tumor necrosis factor- $\alpha$ , lasting until day 9, whereas cytokine level decreased in SSDM-CS-treated group by day 6. Infection exacerbated expression of active matrix metalloproteinases (MMPs)-2 and -9 in controls (day 15), while SSDM-CS positively modulated MMP-2 and -9 with faster decline in their levels (day 12). Inherent nature of the dressing to maintain drug level at equilibrium therapeutic concentration (51.2  $\mu\text{g}/\text{mL}$ ) for prolonged time (72 h), below systemic toxic limits (20  $\mu\text{g}/\text{dL}$ , serum level), accelerated the magnitude and sequence of reparative events. © 2008 Wiley Periodicals, Inc. *J Biomed Mater Res* 89A: 472–482, 2009

**Key words:** silver sulfadiazine; collagen scaffold; *Pseudomonas aeruginosa*; proinflammatory cytokine; matrix metalloproteinases

---

## INTRODUCTION

Wound healing is a dynamic, interactive process involving soluble mediators, blood cells, extracellular matrix, and parenchymal cells.<sup>1</sup> These phases are altered from their normal sequence in the case of infection. Pathogenic microbes, especially *Pseudomonas aeruginosa*, induce pathogenicity because of extracellular virulence factors, which exacerbate the immunocompromised state induced by burn injury.<sup>2</sup> Virulence factors trigger serious weight loss, delay reepithelialization, causes early dehiscence, alters collagen content, impede epidermal migration, and also spread systemically leading to sepsis.<sup>3–6</sup> Further, they induce the production of proinflammatory cytokines, viz, interleukin-1 $\beta$  (IL-1 $\beta$ ), tumor necrosis factor- $\alpha$  (TNF- $\alpha$ ), and IL-6.<sup>7</sup> These cytokines play a major role in regulation of immune response, hematopoiesis, and inflammatory reactions.<sup>8</sup> Among these

cytokines IL-6 has short peak time in normal healing process, whereas IL-1 $\beta$  and TNF- $\alpha$  are shown to persist for longer time.<sup>9–11</sup> Another major detrimental factor to healing process is the altered expression pattern of metalloproteinases (MMPs), which impedes epidermal migration, and degrades all components of extra cellular matrix (ECM) with broad and overlapping specificities.<sup>12–14</sup>

Despite the systemic antibiotic therapy, prevention of infection at the wound site greatly influences the inflammatory and remodeling events. Topical treatment offers the advantage of immediate effect by lowering systemic levels and increasing local tissue bioavailability. Of all the antibacterials available for topical application, silver sulfadiazine (SSD) is the drug widely used. SSD is an oligodynamic antimicrobial, in which  $\text{Ag}^+$  component, even in small amounts, exerts an antimicrobial effect in deep burn injury.<sup>15</sup> Later, it was found that silver gets absorbed systemically posing problems on prolonged use. Controlled delivery system developed by us maintains therapeutic level of SSD, which remains below toxic limits. In this system, reconstituted collagen scaffold impregnated with SSD-loaded alginate

Correspondence to: M. Babu; e-mail: marybabu@hotmail.com or babumary2000@yahoo.com

microspheres was developed to deliver the drug in a controlled manner. The antibacterial efficiency against *P. aeruginosa* showed minimal bactericidal concentration level of 51.2 µg/mL and the system was able to control infection for extended time period with lesser dressing frequencies and easier assessment of wound.<sup>16</sup>

The present *in vivo* experiment is aimed at investigating the efficiency of silver sulfadiazine from collagen scaffold (SSDM-CS) on deep second degree burn wounds challenged with *P. aeruginosa*. Immunohistochemical localization of proinflammatory cytokines and quantitative assessment of collagen turn over, tissue level expression of MMP-1, MMP-2, and MMP-9 were performed. The influence of early infection on various cascading phases during healing process has been analyzed with special reference to efficient granulation tissue formation and effective remodeling.

## MATERIALS AND METHODS

### Materials

Hydroxyproline, Glucosamine HCl, *para*-dimethyl amino benzaldehyde, acetyl acetone, chloramine-T, bicinechonic acid, bovine serum albumin, MMP-2 (EC 3.4.24.24), and MMP-9 (EC 3.4.24.35) from human fibroblasts, alkaline phosphatase (AP) chromogen-Nitro Blue Tetrazolium (NBT), 5-bromo,4-chloro,3-indolylphosphate (BCIP), and fast red substrate were from SIGMA, USA. Primary antibodies used were mouse monoclonal anti-MMP-1, goat polyclonal anti-MMP-2 and MMP-9, polyclonal rabbit anti-IL-1β, IL-6, and TNF-α. Monoclonal rabbit anti-mouse IgG-AP, and polyclonal donkey anti-goat IgG-AP secondary antibodies were used to probe MMP-1 and MMP-2 and -9, respectively. For immunohistochemical localization AP-tagged monoclonal goat anti-rabbit IgG was used. All antibodies used were from Santa Cruz Biotechnology, CA. Mueller Hinton Broth and Mueller Hinton Agar were obtained from HI-MEDIA, Mumbai, India and *P. aeruginosa* (ATCC 25619) culture was procured from IMTECH, Chandigarh, India. All other chemicals used for experimental purpose were of analytical grade.

### Methods

#### SSD wound dressing

A reconstituted collagen scaffold impregnated with SSD-loaded alginate microspheres (SSDM-CS), capable of delivering the drug in a controlled manner has been developed as per our previous protocol.<sup>16</sup> Briefly, SSD-loaded alginate microspheres were prepared by modified water-in-oil (w/o) emulsion technique through interfacial ionic gelation of alginate using CaCl<sub>2</sub>. Microspheres of optimum drug entrapment (3.26%) and required size range (300–370

µm) were prepared. SSD release from the scaffold was 68.8% (equilibrium concentration for 72 h) with an initial burst release of 47.5% (≈1.5% of total drug load), whereby therapeutic level of SSD could be attained easily and further maintained for 3 days (the percentage entrapment of SSD obtained through our process was optimal as it complies with USP standard,<sup>17</sup> which recommends 1.5% of SSD for topical dosage forms). SSD-loaded microspheres exhibited minimal inhibitory concentration and minimal bactericidal concentration levels of 44.8 and 51.2 µg/mL against *P. aeruginosa* (ATCC 25619).

SSD-loaded microsphere impregnated collagen scaffold was then developed by adding a known amount (0.5 g) of SSD-loaded microspheres to a known amount (300 mg) of pepsin-solubilized collagen<sup>18</sup> and gently stirred to distribute the spheres homogeneously throughout the solution. Following which fibril formation was initiated by adding an appropriate amount of 0.2M phosphate buffer (2 mL) and adjusting the pH to 6.9–7.2 using 2N sodium hydroxide, until turbidity appeared. After fibril formation, the viscous solution was uniformly cast over horizontally placed polypropylene platforms of 10 × 10 × 2 cm<sup>3</sup> dimension. They were allowed to dry at a constant temperature of 34°C until a thin scaffold was obtained. The scaffold was then washed with distilled water twice or thrice to remove excess of salt and completely air-dried and stored in a light proof desiccator for further use.

#### Burn wound model

Female white wistar rats, weighing 180–220 g were procured from Tamil Nadu Veterinary University, Chennai, India (TANUVAS) and acclimatized to laboratory conditions for 1 week. They were fed with standard rat chow and tap water *ad libitum*. Institutional animal ethical committee approved all the animal experiment protocols. Animal maintenance and care were according to the Committee for the Purpose of Control and Supervision of Experiments on Animals guidelines, India.

Deep second degree burn wound was created by an instrument designed by us using commercially available solder rod (500 g) (Fig. 1). The edge of the solder rod was cut and replaced by a circular iron disc of thickness 1.25 cm and diameter of 3 cm. A thermal sensor was connected to the non-contacting surface and the temperature was observed through a digital read-out. The desired temperature was attained by electrically heating the solder rod and temperature was controlled using a thermostat. Before creation of burn wound, rats were anaesthetized by intraperitoneal injection of thiopental sodium (Thiopental), 50 mg/kg body weight. Hair in the dorsal side of the rats were removed and burn wound was inflicted by placing the circular iron disc (heated to 82–85°C) over the dorsal side for 20 s, without exerting any external pressure.

#### Experimental design

Rats were randomly divided and assigned equally ( $n = 30$ ) to one of the following groups, group 1—noninfected controls dressed with saline gauze, group 2—noninfected rats treated with SSDM-CS, group 3—infected controls

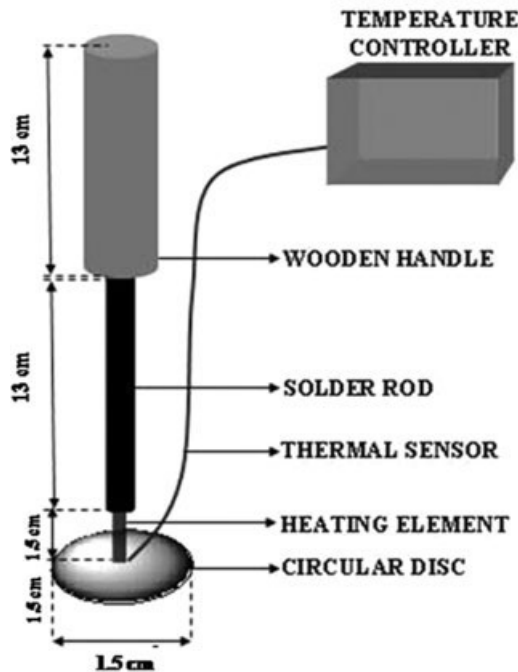


**Figure 1.** Schematic diagram of modified solder unit used for infliction of burns.

challenged with *P. aeruginosa* infection and dressed with saline gauze, and group 4—infected rats treated with SSDM-CS. The dressing was changed after every 3 days, from day 1.

#### Bacteriological methods

Pathogenic strains of *P. aeruginosa* (ATCC 25619) was grown on Mueller Hinton Broth at 35°C until logarithmic growth phase ( $\approx 0.5$  McFarland)<sup>19</sup> and approximately diluted to prepare the bacterial challenge inoculum [ $10^7$  colony forming units (cfu)/mL]. For inducing infection, 1 mL of the above inoculum was centrifuged and resuspended in 100 mL of sterile saline and the suspension was injected carefully between the subcutaneous skin and paraspinus muscular layer.<sup>20</sup> Rats with wounds colonized with  $\geq 10^6$  cfu (assessed quantitatively by spread plate method from the tissue extract prepared from biopsy of 1 cm<sup>2</sup> with 1 mL of sterile saline) and showing positive infiltration of deep dermal neutrophils after 12 h of bacterial challenge were included in the study. The severity of the infection in groups 3 and 4 was assessed at regular time intervals and represented as cfu/ml (after extracting biopsy tissue with 1 ml of sterile saline).

#### Rate of wound closure

The rate of wound closure was determined by tracing the margin of wound area on to a transparent graph sheet and expressed as percentage surface area reduction at each time interval. At these time intervals changes in body weight was recorded, granulation tissue was collected from each group, and serum from blood samples of

SSDM-CS-treated groups (2 and 4) were collected and subjected to further analysis.

#### Determination of collagen and hexosamine content

A known amount of granulation tissue (5 mg) was collected at regular time intervals, freeze-dried (Yamato, Japan) to constant weight, and subjected to hydrolysis for 22 h with 6N HCl to determine the collagen content.<sup>21</sup> Total hexosamine content was determined by the method of Elson and Morgan<sup>22</sup> after subjecting the samples to hydrolysis for 6 h using 2N HCl.

#### Immunohistochemical analysis

The early and late course of inflammatory response during healing was observed by the proinflammatory cytokines IL-1 $\beta$ , IL-6, and TNF- $\alpha$  expression. Immunohistochemistry was performed according to earlier procedure.<sup>9</sup> The sections of post-burn days (until day 12) were incubated for 1–2 h at 37°C, individually with polyclonal rabbit primary antibody for IL-1 $\beta$ , IL-6, and TNF- $\alpha$  (1:100 in 2% bovine serum albumin) followed by incubating the sections with AP-tagged anti-rabbit IgG (1:200 dilutions) for 45 min to 1 h at 37°C. Then, sections were stained with fast red substrate (prepared with buffer provided in the kit by manufacturers), after washing overnight in water (in dark). Finally, they were counterstained with Mayer's Hematoxylin for 15 min and mounted using crystal mountant.

#### Determination of MMP expression pattern

Expression of active MMPs in granulation tissue of burn wounds of all the groups at various time intervals was determined by gelatin zymography, whereas both active and inactive forms combined were determined by western blot analysis.

#### Gelatin zymography

In the investigation, the expressions of MMP-2 and -9 at various time intervals in all the groups were analyzed. Granulation tissue lysate was obtained through extraction with 20 mM HEPES buffer, pH 7.2, at 4°C. Before zymography, the protein concentration in the samples were determined through Bicinchoninic acid assay.<sup>23</sup> Samples of equal protein content (20  $\mu$ g) were mixed with nonreducing Laemmli's buffer (0.125M Tris, pH 6.8, SDS 4%, glycerol 20%, and 0.02% w/v of bromophenol blue) and electrophoresed on a 10% polyacrylamide gel copolymerized with gelatin (1 mg/mL). Standard MMP-2 and -9 were used as markers. After electrophoresis, the gel was washed with 2.5% of Triton X-100 for 1 h and 30 min and then incubated with enzyme buffer (50 mM of Tris-HCl, 150 mM NaCl, 5 mM CaCl<sub>2</sub>, and 0.05% sodium azide) at 37°C for 20 h to allow reactivation of MMP. Gels were then stained with 0.5% of Coomassie Brilliant Blue R-250<sup>24</sup> and destained with 10%v/v of acetic acid containing 30%v/v of methanol. The MMPs were visualized as clarified bands corresponding to zones of digestion of substrate gelatin.

## Western blot analysis of MMPs

Tissue lysate of all groups collected at various time intervals, containing equal amount of protein (20  $\mu$ g) were mixed with Laemmli's reducing buffer and subjected to electrophoresis on a 10% polyacrylamide resolving gel. After resolving the protein bands, they were transferred to nitrocellulose membrane (Millipore, USA) using BioRad minigel Transfer apparatus, for 1 h and 30 min, and were incubated with primary antibody for MMP-1, -2, and -9, individually at 4°C for 16 h. After incubation, blots were washed with PBS containing 0.5% Tween 20 and then incubated with respective AP-conjugated secondary antibodies for 1 h and visualized using NBT/BCIP (33:66  $\mu$ L in 10 mL of AP buffer) as a chemiluminescence substrate.<sup>25</sup> The immunoblots were subjected to densitometric analysis (BioRad densitometric Geldoc XR image acquisition equipped with quality one software for 1D electrophoretic analysis) to quantitate the total MMP expression (both active and pro forms of MMP). The images were photodocumented by integrating the volume of each band after background corrections. The volume intensities were analyzed through the volume analysis tool, where the volumograms were calculated in terms of pixels and plotted against different time intervals. Each MMP was individually subjected to analysis twice by western blot and the volumograms of two immunoblots are represented as mean number of pixels  $\pm$  SD and statistically analyzed (mentioned below).

## Determination of silver content in serum

Serum samples of known volume (1 mL) were digested with 5 mL of 0.2N nitric acid and residue was made up to a standard volume. Silver content in the samples was estimated using atomic absorption spectrophotometer (Spectra varian Atomic Absorption Spectrophotometer, USA) in flame mode using an auto sampler. Back ground corrections were operated at lamp current of 4 mA, slit width of 0.5 nm, and at a wavelength of 328.1 nm.

## Statistical analysis

All graphical illustrations in this study are represented as mean  $\pm$  SD and analyzed with one-way analysis of variance using the Microsoft Excel statistical analysis tool pack. Wherein, variance within each group was compared individually and also against two, three, and all groups combined together. Test for significance was performed with confidence limit of 95%, i.e.,  $p < 0.05$  was considered statistically significant.

## RESULTS

The present investigation deals with several responses in magnitude and temporal pattern of wound repair in *P. aeruginosa* (ATCC 25619) challenged deep second-degree burn model in rats. It was observed that there exists a strong relationship

between the severity of early infection and subsequent healing events. The wound depth was assessed by staining the histological sections of burn tissue with Hematoxylin and Eosin<sup>26</sup> (data not shown).

## Wound closure

The efficiency of SSDM-CS against microbial challenge was assessed by observing the wound healing pattern in treated rats, in comparison with their respective controls. There was an observable increase in wound size till day 6 in all the groups (Fig. 2). The noninfected control group (group 1), showed an increase in wound size till day 12, after which a constant decrease was observed with complete healing occurring by day 30 (99%). On the other hand noninfected SSDM-CS-treated group (group-2) exhibited a significant decrease in wound size as early as day 9 showing complete healing by day 21.

In contrast, infected rats (group 3) showed a significant increase in wound size till day 15, followed by a positive healing, which was slow when compared with other groups and complete closure was observed by 37 days. Infected rats (group 4) treated with SSDM-CS showed an increase in wound size till day 9, after which it exhibited positive healing response achieving complete healing by day 27. It is observed that group 3 (infected controls) exhibited significantly larger wound size against other groups at all time points (group 3 vs. groups 1, 2, and 4;  $p < 0.05$ ). The healing pattern in groups 1 and 4 is similar from day 12 until day 18. During this time course the wound size was statistically insignificant

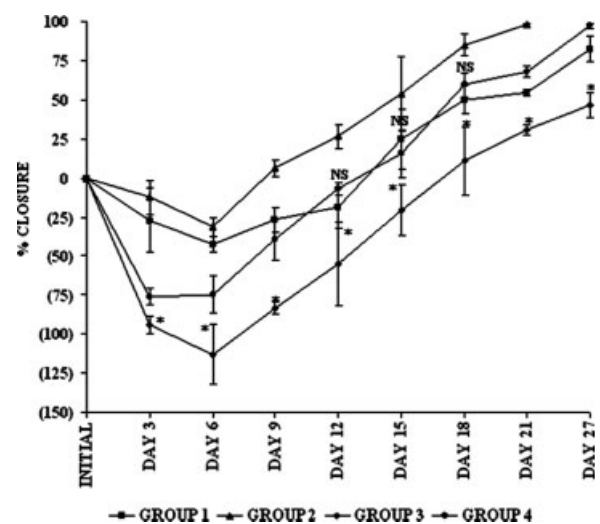


**Figure 2.** Graph showing percentage wound closure observed over 27 days in both infected and noninfected groups treated with SSDM-CS in comparison with their respective controls. Y-axis values in brackets indicates increase in percentage wound size. \* $p < 0.05$ , group 3 vs. group 1, 2, and 4. NS, not significant, group 4 vs. group 1.

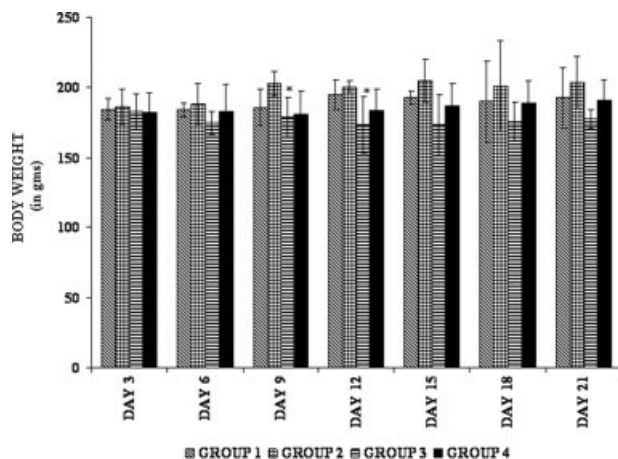


**Figure 3.** Comparison of changes in body weight observed in various groups: \* $p < 0.05$ , group 3 vs. group 4.

(group 1 vs. group 4,  $p = 0.237$ ), after which healing was observed to be faster in group 4 with significant difference until day 27 ( $p = 0.0162$ ). Similarly, when noninfected groups were compared (group 1 vs. group 2) the healing rate matched on day 15, which was statistically insignificant, after which group 2 showed faster healing.

### Body weight assessment

The average body weight of the rats ( $n = 120$ ) was 184 g. Comparison within noninfected and infected groups did not show any significant ( $p < 0.05$ ) weight loss over a period of 21 days (Fig. 3). The weight of the noninfected controls remained same until day 9, after which an increase of 4% from initial weight was observed. In contrast, the infected control group (group 3) showed a constant decrease (5%) from their initial weight till day 15, after which only a marginal increase was seen but they did not attain the initial weight until complete healing. In SSDM-CS-treated infected rats (group 4) there was marginal weight loss (1%) initially but they regained their initial weight and showed an increase of 3% from their original body weight. When the comparison was made between groups 1, 2, and 4 there was variation in the weight, which was not statistically significant. But the infected control showed a significant difference against the noninfected groups [day 9 ( $p = 0.0247$ ) and day 12 ( $p = 0.0401$ )] (group 3 vs. groups 1 and 2).

### Influence of infection on healing

Groups 3 and 4 rats infected with *P. aeruginosa* ( $10^7$  cfu) exhibited differential microbial load during

the course of healing. On day 3, group 3 showed a significant increase in cfu (from  $2 \times 10^7$  cfu to  $10^9$  cfu, microbial count determined in the slough of the wound since granulation was not obtained), whereas SSDM-CS-treated rats did not show a significant increase or decrease (from  $2 \times 10^7$  to  $4 \times 10^7$  cfu) (Fig. 4). However, on day 6, group 4 showed a significant decrease in microbial load (from  $4 \times 10^7$  to  $2 \times 10^4$  cfu), which constantly reduced on post-burn days. Group 4 showed 99.9% decrease by day 9 (reduction of microbial load from  $10^7$  to  $10^2$  cfu), but group 3 did not exhibit any significant decrease till day 15. Almost 75% of group 3 showed mild to severe purulent discharge, indicating the onset of positive infection. The severity of infection was obvious in group 3, leading to mortality of 3 animals, indicating that local infection has detrimental effect on healing.

### Collagen and hexosamine content

Initial collagen expression levels are significantly different between groups 1, 2, and 4 ( $p = 0.00024$ , on day 3). No significant difference was observed when collagen turnover was compared within the noninfected groups (Fig. 5). It is interesting to note that SSDM-CS-treated infected group exhibited a significant difference in collagen content until day 12 when compared with infected control (group 4 vs. group 3,  $p = 0.0116$ ), showing peak concentration on day 9. This is much faster than the noninfected controls coinciding with the rate of healing observed (97.12%). Throughout the study, intergroup comparisons exhibited significant differences in collagen content. The noninfected groups (1 and 2) were statistically insignificant when compared with infected group 4 alone (groups 1 and 2 vs. group 4,  $p$ -value

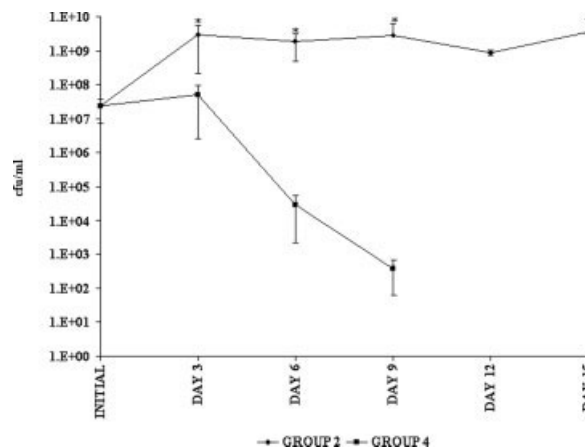


**Figure 4.** Reduction of *P. aeruginosa* cfu observed in SSDM-CS rats (group 4) in comparison with infected controls (group 3). \* $p < 0.05$ , group 3 vs. group 4.

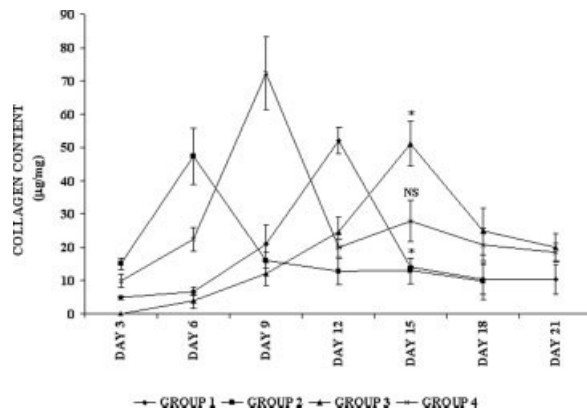


**Figure 5.** Collagen content determined in granulation tissue collected from infected and noninfected group rats treated with SSDM-CS in comparison with their respective controls at various time intervals. \* $p < 0.05$ . NS, not significant, group 4 vs. groups 1 and 2.

was within level of confidence, 95%). The groups are ranked with respect to their matrix deposition, based on collagen turn over as follows, group 2 > group 4 > group 1 > group 3. Proteoglycans deposition mainly hyaluronic acid, heparan sulfate, chondroitin sulfate, and dermatan sulfate in granulation tissue facilitates an environment for cell movement and collagen deposition. Hexosamine (markers of proteoglycan) expression is significant in all groups (Fig. 6) till day 12 ( $p < 0.05$ ), after which there was no significant difference between the groups ( $p < 0.05$  and  $< 0.01$ ). Peak concentrations were 2-fold lower in infected groups (2.83  $\mu\text{g}/\text{mg}$  on day 12 for group 3 and 2.206  $\mu\text{g}/\text{mg}$  on day 9 for group 4) in comparison with the noninfected groups (4.15  $\mu\text{g}/\text{mg}$  on day 9 for group 1 and 4.45  $\mu\text{g}/\text{mg}$  on day 6 for group 2) and there was only a marginal increase within the groups, indicating less deposition of matrix in infected groups.

### Influx of proinflammatory cytokines

Proinflammatory cytokines, IL-6, IL1- $\beta$  and TNF- $\alpha$  influence the healing process by modulating the level of MMPs. A varied expression pattern of these cytokines was observed between treated and untreated groups, as well as with respect to infection status. The control groups exhibited increased expression of IL1- $\beta$  when compared with their respective treated groups [Fig. 7(A)]. Especially in group 3, persistent expression was seen until day 9, while group 4 treated with SSDM-CS showed lesser expression, which subsided by day 6. Another proinflammatory cytokine IL-6, which generally shows a steep increase in its level during initial inflammatory phase and quickly declining within short time, was persistent and widespread over dermal regions until

day 6 in group 3 [Fig. 7(B)]. Whereas in group 4 and group 1 expression of IL-6 was marginal and subsided by day 3, indicating its transient expression. TNF- $\alpha$  a key mediator of late inflammatory phase is generally expressed in cases of severe infection. Group 3 showed predominant expression of TNF- $\alpha$  till day 9, whereas in other groups its expression subsided within 6 days [Fig. 7(C)]. Especially, SSDM-CS treated groups (2 and 4) exhibited low level of expression in comparison with their respective controls, indicating the ability of SSDM-CS to mitigate infection.

### Differential expression of matrix MMP

#### Detection of active MMPs by gelatin zymography

Expression of pro- and active forms of MMP-2 and -9 in the granulation tissues of post-burn days shows relative changes over time (Fig. 8). Group 1 showed higher levels of both pro- and active form of MMP-2 and -9 on day 3, whereas on day 6 the expression of active form was more than the proform. It is also observed that overall expression of MMP-2 was lesser than MMP-9. Noninfected treated group (group 2) showed a proportionate decrease in MMP-2 and -9 over time, but at a faster rate than group 1. A distinct feature is the absence of MMP-2 expression from day 9 and the levels were comparatively low (on day 3) in group 2 than in group 1. In comparison with the noninfected group, the overall expression of both MMP-2 and -9 in infected group were significantly lower, thus hindering active remodeling. The expression of both MMP-9 and -2, though less, can be observed for longer duration in case of infected group (group 3), until day 18. Whereas group 4 rats (SSDM-CS treated) showed

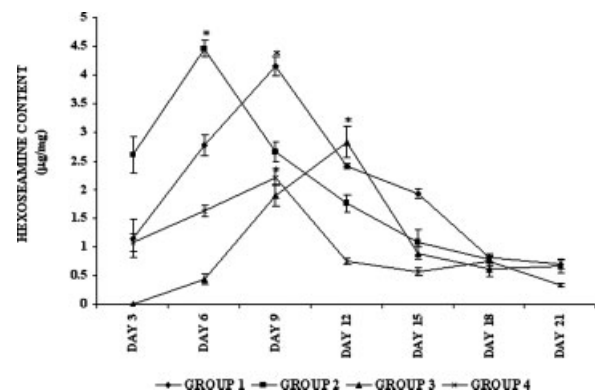


**Figure 6.** Total hexoseamine content determined in granulation tissue of infected and noninfected rats treated with SSDM-CS in comparison with their respective controls at various time intervals. \* $p < 0.05$ , groups 3 and 4 vs. groups 1 and 2. (infected vs. non-infected).

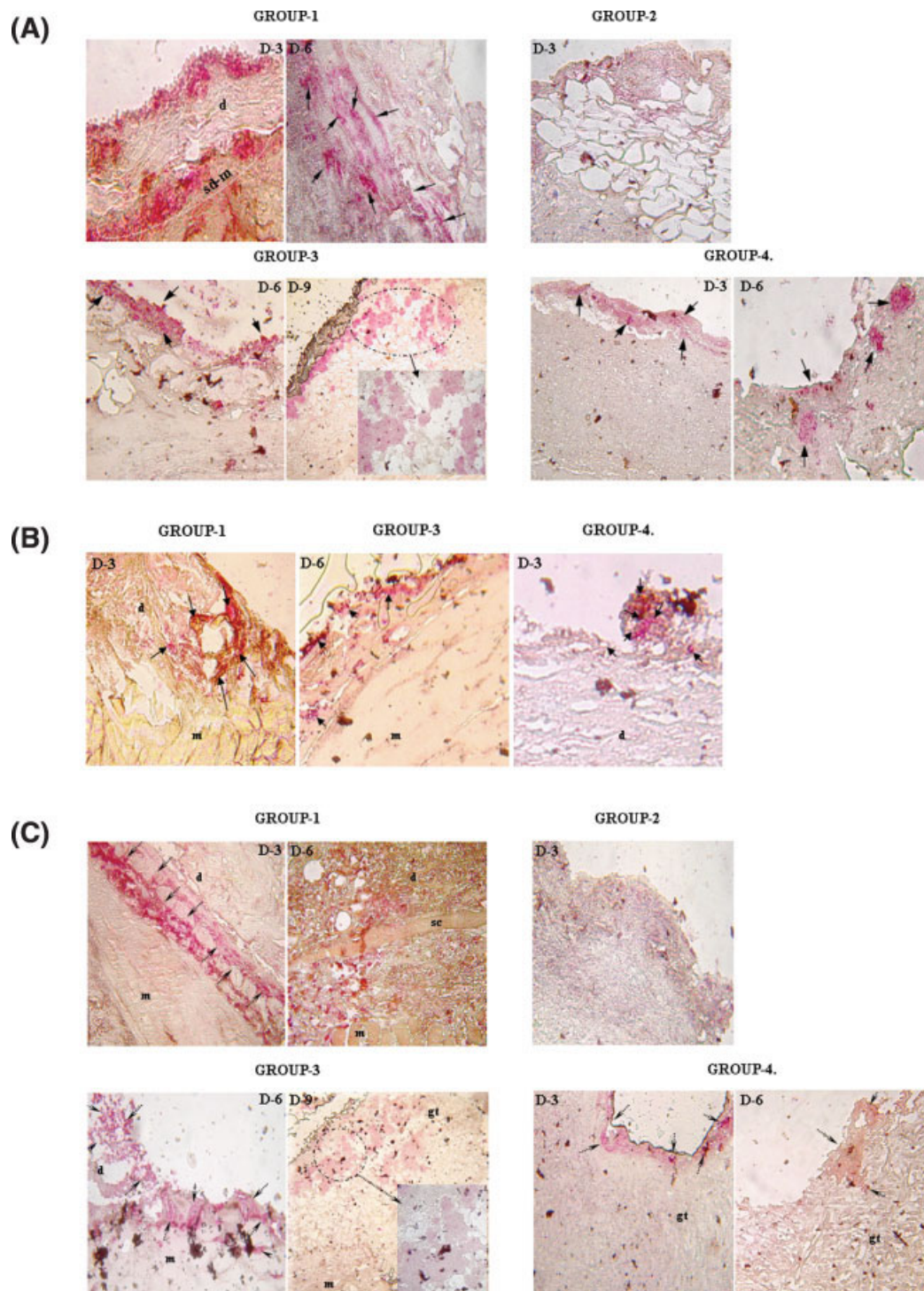


**Figure 7.** Immunohistochemical localization of proinflammatory cytokines in granulation tissue. (A) Expression of IL-1 $\beta$  (bold arrow) detected in granulation tissue of various groups, at dermal (d) and sub-dermal-muscular junction (sd-m). Inset on day 9 photograph of group 3 shows magnified image of cellular infiltration of IL-1 $\beta$ . (B) Expression of IL-6 (bold arrow) seen on disrupted dermal regions (d), Expression can be observed even in muscle layer (m) of infected controls (group 3). (C) Expression of TNF- $\alpha$  (bold arrows) observed in various groups in dermal (d) regions that spreads sparsely over muscular (m) and subcutaneous (sc) layers. Inset on day 9 photograph of group 3 shows cellular infiltration of TNF- $\alpha$ . gt, granulation tissue. [Color figure can be viewed in the online issue, which is available at [www.interscience.wiley.com](http://www.interscience.wiley.com).]

appreciable levels of expression of MMPs until day 6, after which MMP-2 levels declined, while MMP-9 expression could be still observed. After day 12, expression of both MMPs in group 4 diminished,

which can be attributed to the control of microbial burden from day 9. Expression of MMP-9, in group 3, even on day 15, indicates slower onset of remodeling.

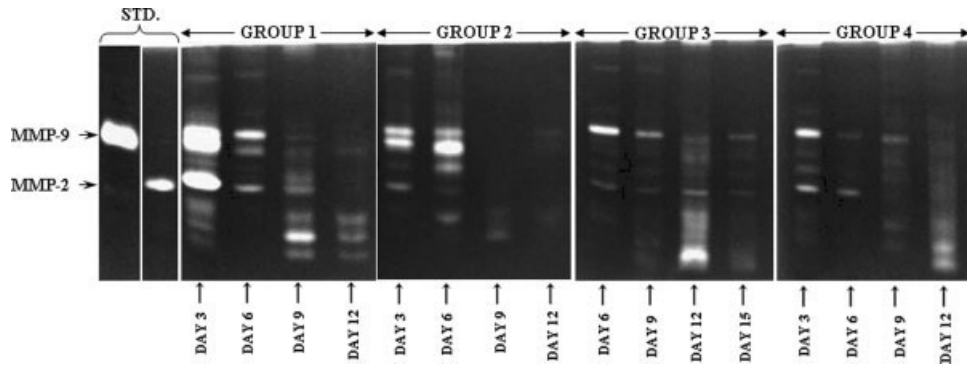


**Figure 8.** Differential expression of active MMP-2 and MMP-9 observed through gelatin zymography of granulation tissue extract on various post-burn days.

Analysis of matrix MMP by western blot

MMPs are present along with tissue inhibitors of MMP that may not be detected by zymography. Young and Grinnell<sup>27</sup> have provided evidence for detecting both active and inactive forms MMPs through western blot analysis and shown it to give a measure of total MMPs expressed. Hence in this study total expression of MMP-2 and -9 were analyzed through western blot (Fig. 9).

Volumograms of MMP-1, MMP-2, and MMP-9 by densitometry (Fig. 10) exhibited both active and inactive forms of enzymes at various post-burn days. MMP-1 levels were found to be high during initial days of healing (3–6) in all the groups [Fig. 10(A)]. MMP-1 linearly decreased with time in both the non-infected groups, whereas level of expression showed variation in both the infected groups. Group 4 exhibited significant increase in MMP-1 levels until day 9 (group 4 vs. groups 1 and 2) and it decreased

on par with the noninfected group, which was statistically insignificant ( $p = 0.05293, p < 0.05$ ). Comparison within groups does not show significant level of expression of MMP-1 on day 15 (group 1 vs. group 2,  $p = 0.0881$  and group 3 vs. group 4,  $p = 0.1389$ ). In groups 1, 2, and 4, expression of MMP-2 [Fig. 10(B)] increased gradually with time till day 9, after which it rapidly declined, whereas infected control group showed variable expression levels until day 18. Rats in group 4 (SSDM-CS treated) exhibited higher levels of MMP-2 until day 9 and the level significantly decreased from day 12 onward in comparison with group 1 ( $p = 0.0013$ ). MMP-9 expression was high during initial days in all the groups [Fig. 10(C)]. Infected groups (3 and 4) exhibited high level of expression than the noninfected groups throughout the study. It can be observed that group 3 exhibited  $\approx 2.5$ -fold higher levels in comparison with other groups and its expression was observed even on day 18.

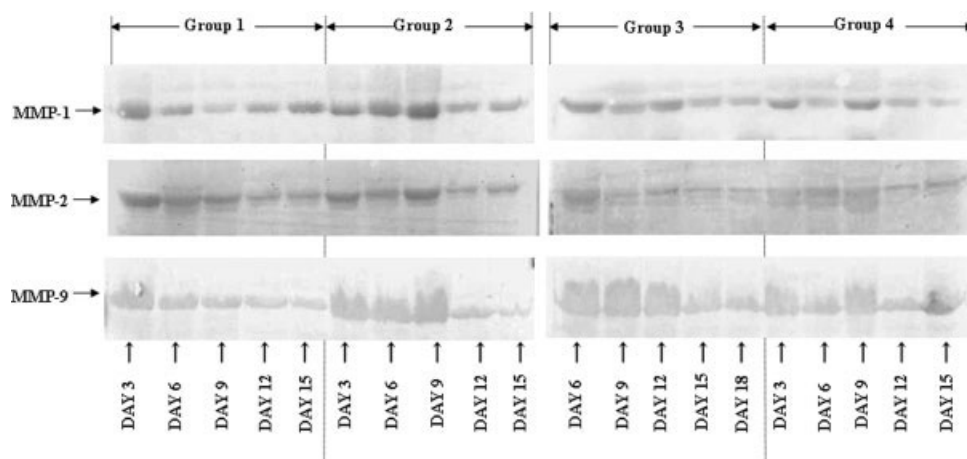


**Figure 9.** Western blot analysis of both active and inactive MMP-1, MMP-2, and MMP-9 levels in various post-burn days.



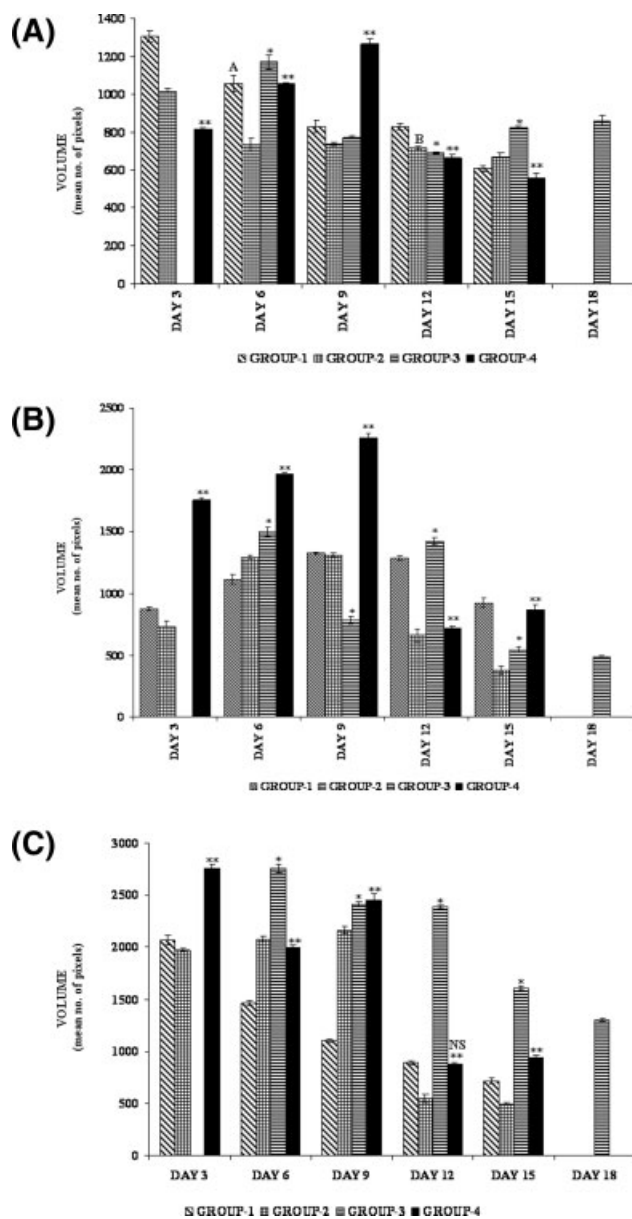


**Figure 10.** Densitometric analysis of MMP-1, MMP-2, and MMP-9 levels observed in western blots. (A) Comparison of MMP-1 levels observed in infected and noninfected rats treated with SSDM-CS in comparison with their respective controls at various time intervals.  $p < 0.05$ , \*group 3 vs. groups 1 and 2, \*\*group 4 vs. groups 1 and 2. (a)  $p < 0.05$ . NS, not significant on day 6, groups 3 and 4 vs. group 1. (b)  $p < 0.05$ . NS, not significant on day 12, groups 3 and 4 vs. group 2. (B) Comparison of MMP-2 levels observed in infected and noninfected rats treated with SSDM-CS in comparison with their respective controls at various time intervals.  $p < 0.05$ , \*groups 1 and 2 vs. group 3, \*\*groups 1 and 2 vs. group 4. (C) Comparison of MMP-9 levels observed in infected and noninfected rats treated with SSDM-CS in comparison with their respective controls at various time intervals.  $p < 0.05$ , \*group 3 vs. groups 1 and 2, \*\*group 4 vs. groups 1 and 2, NS-not significant (group 1 vs. group 4).

Collectively in all the groups, expression of MMP-9 was found to be predominant in comparison with other MMPs. It can be observed from overall expression of various MMPs that there exists a relationship between MMP expression and time of healing in case of groups 1, 2, and 4. These groups exhibit differential expression of various MMPs till day 9, after which a decrease can be observed reaching undetectable low level by day 18. On the other hand, infected control group (group 3) showed variation in the expression of all MMPs at all time periods. Hence, it is evident that the microbial load greatly influences remodeling event.

## DISCUSSION

Despite major advances in burn wound management and other supportive care regimen, infection remains the leading cause of morbidity and mortality. The burn wound created in this study by the instrument designed, was deep second degree and vulnerable to infection. Hence, the subcutaneous injection of  $10^7$  cfu/mL of *P. aeruginosa* caused severe infection and its importance was shown in previous studies.<sup>28</sup> Severe infection caused an enlargement of wound size during initial days in both infected and noninfected groups, in particular the infected rats showed an increase (>50%) in size, implicating the effect of infection on healing process. Infection also caused hypermetabolic response by affecting the nutritional balance and directly influencing the body weight.<sup>29</sup> The infected rats (groups 3 and 4) showed reduction in body weight, which was significant in group 3 when compared with groups 1 and 2 on day 9, whereas group 4 rats did not show any significant weight loss. The later group started to regain the body weight once the microbial load receded (after 9 days), because SSDM-CS treatment exerted antimicrobial effect through controlled delivery of SSD. A further evidence for this effect was the sharp reduction from  $10^7$  to  $10^2$  cfu by day 9 in group 4 and increase in percentage wound closure on par with noninfected control, exhibiting faster healing (15% more reduction in wound size on day 27).

A significant feature of thermal burn is slow re-epithelialization in both early and later time points because of loss/damage of follicles residing in deep dermal regions. Bacterial load aggravates the damage by gaining entry through the follicular path; reside deep in the follicular-basement juncture and further infiltrates into deep dermal and paraspinal muscular layers. This is of paramount importance since keratinocytes use the same portal for re-epithelialization.<sup>30</sup> Though the normal wounds and

infected wounds share similar process of granulation characteristics, existence of large bacterial load in infected rats exerted a detrimental effect on rate of granulation and re-epithelialization. Both groups 3 and 4 showed existence of infection during early days of healing, sequentially affecting epidermal maturation. After day 9 group 4 exhibited significant proliferation and migration of epidermal cells over fibrin matrix and looked similar to groups 1 and 2, resulting in faster granulation covering the entire wound surface. Whereas, infected control showed poor granulation over a long time ( $\geq 18$  days) because of persistent infection. Another striking feature is the appearance of spongy collagen layer as early as day 15 in group 2 rats, and on day 21 in case of group 4 rats, while group 1 rats exhibited striated fibrillar appearance on day 27. Faster collagen deposition in SSDM-CS-treated rats, in comparison with their respective controls, attributed to faster cellular infiltration and fibroblasia. Glycosaminoglycan content also reached the maximum at faster rate in the treated groups indicating better remodeling.

Another vital event during burn wound healing is inflammatory response, which is aggravated due to infection. Early onset of proinflammatory cytokines, IL-6, IL-1 $\beta$ , and TNF- $\alpha$  demonstrates the wound status and especially persistent expression of IL-1 $\beta$  and TNF- $\alpha$  provides ample evidence for severity of infection in triggering inflammatory response. In normal healing process, IL-6 expression reaches the peak level rapidly and declines, whereas expression of IL-1 $\beta$  and TNF- $\alpha$  can be observed for longer time. The immunohistochemical analysis shows prolonged expression of IL-6 (day 6) along with IL-1 $\beta$  and TNF- $\alpha$ , in infected control, indicating the severity of inflammation. Whereas, SSDM-CS treatment gives normal expression of proinflammatory cytokines similar to noninfected controls.

Prolonged expression of MMPs is likely to cause destruction of the early provisional matrix, which was further exacerbated due to heavy microbial load in group 3, whereas SSDM-CS-treated groups exhibited better remodeling due to positive modulation of MMPs. Early expression of MMPs in groups 1, 2, and 4 indicates the active clearance of dead tissue in these groups. Though the magnitude of expression varied within groups 1 and 4, the pattern of expression was found to be consistent. Another important observation is the delayed onset and prolonged expression of MMP 1, 2, and 9 in infected controls. One of the major factors that regulate MMP activity is the bacterial exotoxins<sup>31</sup> along with excessive inflammatory cell infiltration at the wound site. In addition regulation of MMP-tissue inhibitor of MMP association during healing process plays a crucial role in matrix remodeling.<sup>12</sup> The SSDM-CS reduces the bacterial load and found to lower the proinflam-

matory cytokines thus positively modulating MMP activity.

The results of the current investigation affirm the influence of infection on healing events and its response to controlled delivery of SSD. Perhaps this seems to be the first report to show the controlled delivery of SSD through collagen dressing to control early onset of infection, and the subsequent events. This report correlates well with the previously suggested hypothesis<sup>32</sup> that controlled delivery of silver is effective in the healing process by modulating the overall MMP activity.

From silver incorporated dressings, when Ag<sup>+</sup> ions are released in bolus there is a possibility that Ag<sup>+</sup> binds with serum proteins and chloride ions present in the wound fluids. This causes quick inactivation of a large portion of Ag<sup>+</sup> as well as causes accumulation of Ag<sup>+</sup> ions elsewhere in the body through systemic circulation, whereas SSDM-CS treatment maintains steady state equilibrium of drug at therapeutic levels. These results correlate well with our previous *ex vivo* release profiles.<sup>16</sup> Through serum analysis, we have proved that silver concentrations were below the toxic limits 20  $\mu\text{g}/\text{dL}$  (silver analysis in serum was below detectable limits).<sup>33</sup> Earlier dressings developed were mainly with synthetic polymers and do not give clear evidence in controlling its release from the base dressing material. Recently, silver ions coated dressing has been developed and evaluated for its ability to control infection silver concentrations at low levels.<sup>34</sup> In these dressings Ag<sup>+</sup> are coated on the basis of charge interaction. Hence, when applied *in vivo* these silver ions are released due to change in electrostatic flux. Recent proposition to deliver silver ions in a sustained fashion through polyethylene glycol based system has presented no adverse effect on cell migration or proliferation.<sup>35</sup> Evidence has been provided for their ability to effectively kill the pathogens that causes infection *in vitro*. Moreover, incorporation of collagen type I into the polymer corrected the impaired cell migration.<sup>35</sup>

## CONCLUSION

Collectively, the present model is designed taking into account the situations where infection in burns are severe and significantly affecting healing bearing in mind the narrow toxicity limit (20  $\mu\text{g}/\text{dL}$ ) of SSD when used for prolonged period *in vivo*, providing a close simulation with respect to clinical setting. This investigation also reveals that control of inflammation and MMP regulation depends on the therapeutic efficacy of the initial chemoprophylaxis applied to control infection. In addition, it would be a constructive proposition if the wound dressing product

could assist in controlling the proteolytic wound environment for accelerated remodeling and wound closure.

One of the authors, N. S., thank the Department of Biotechnology (DBT) for providing fellowship. We express our sincere thanks to Dr. A. B. Mandal, Director, CLRI for giving us the opportunity and encouragement to carry out the work.

## References

- Singer AJ, Clark RAF. Cutaneous wound healing. *N Engl J Med* 1999;341:738–746.
- Stieritz DD, Holder IA. Experimental studies of pathogenesis of infections due to *Pseudomonas aeruginosa*: Description of a burned mouse model. *J Infect Dis* 1975;131:688–691.
- Steinstraesser L, Burkhard O, Fan MH, Jacobsen F, Marcus L, Su G, Daigler A, Steinau HU, Remick D, Wang SC. Burn wounds infected with *Pseudomonas aeruginosa* triggers wight loss in rats. *BMC Surg* 2005;5:1–7.
- Smith M, Enquist IF. A quantitative study of impaired healing resulting from infection. *Surg Gyn Obstet* 1967;125:965–973.
- Robson MC. A failure of wound healing caused by an imbalance of bacteria. *Surg Clin N Am* 1997;77:637–650.
- Singer AJ, McLain SA. Persistent wound infection delays epidermal maturation and increased scarring in thermal burns. *Wound Repair Regen* 2002;10:372–377.
- Freudenberg MA, Ness T, Kumazawa Y, Galanos C. The role of cytokines in endotoxic shock and in endotoxin hypersensitivity. *Immun Infekt* 1993;21:40–44.
- Reddy RC, Chen GH, Tekchandani RK, Standiford TJ. Sepsis-induced immunosuppression: From bad to worse. *Immunol Res* 2001;24:273–287.
- Moulin V. Growth factors in skin wound healing. *Eur J Cell Biol* 1995;68:1–7.
- Neely AN, Hoover DL, Holder IA, Cross AS. Circulating levels of Tumour Necrosis Factor, Interleukin 6 and proteolytic activity in a murine model of burn and infection. *Burns* 1996;22:524–530.
- Grellner W. Time-dependent immunohistochemical detection of proinflammatory cytokines (IL- Beta, IL-6, TNF-Alpha) in human skin wounds. *Forensic Sci Int* 2002;130:90–96.
- Armstrong DG, Jude EB. The role of matrix metalloproteinases in wound healing. *J Am Podiatr Med Assoc* 2002;92:12–18.
- Werb Z. ECM and cell surface proteolysis: Regulating cellular ecology. *Cell* 1997;9:1439–1442.
- Shapino SD. Matrix metalloproteinases degradation of extracellular matrix: Biological consequences. *Cell Biol* 1998;10:602–608.
- Monafo WW, Freedman B. Topical therapy for burns. *Surg Clin North Am* 1987;67:133–145.
- Shanmugasundaram N, Sundaraseelan J, Uma S, Selvaraj D, Mary Babu. Design and delivery of silver sulfadiazine from alginate microspheres-impregnated collagen scaffold. *J Biomed Mater Res B Appl Biomater* 2006;77:378–388.
- Official monograph of silver sulphadiazine cream. USP 24-NF 19;1999. p 1567.
- Fujii T, Kuhn K. Isolation and characterization of pepsin-treated type III collagen from calfskin. *Hoppe Seylers Z Physiol Chem* 1975;11:1793–1801.
- National Committee for Clinical Lab Standards (NCCLS). Methods for dilution antimicrobial susceptibility tests for bacterial that grow aerobically; approved standard, 5th ed, 2000; 20:M7–A5.
- Grzybowski J, Janiak MK, Oldak E, Lasocki K, Wrembel-Wargocka J, Cheda A, Antos-Bielska M, Pojda Z. New cytokine dressings. II. Stimulation of oxidative burst in leucocytes *in vitro* and reduction of viable bacteria within an infected wound. *Int J Pharm* 1999;184:179–187.
- Woessner JF Jr. The determination of hydroxyproline in tissue and protein samples containing small proportions of this imino acid. *Arch Biochem Biophys* 1961;93:440–447.
- Elson LA, Morgan WT. A colorimetric method for the determination of glucosamine and chondrosamine. *Biochem J* 1931;27:1824–1828.
- Smith PK, Krohn RI, Hermanson GT, Mallia AK, Gartner FH, Provenzano MD, Fujimoto EK, Goeke NM, Olson BJ, Klenk DC. Measurement of protein using bicinchoninic acid. *Anal Biochem* 1985;150:76–85.
- Madlener M, Parks WC, Werner S. Matrix metalloproteinases (MMPs) and their physiological inhibitors (TIMPs) are differentially expressed during excisional skin wound repair. *Exp Cell Res* 1988;242:201–210.
- Okada A, Tomasetto C, Lutz Y, Bellocq JP, Rio MC, Basset P. Expression of matrix metalloproteinases during rat skin wound healing: Evidence that membrane type-1 matrix metalloproteinase is a stromal activator of pro-gelatinase A. *J Cell Biol* 1997;137:67–77.
- Watts AM, Tyler MPH, Perry ME, Roberts AHN, McGrouther DA. Burn depth and its histological measurement. *Burns* 2001;27:154–160.
- Young PK, Grinell F. Metalloproteinases activation cascade after burn injury: A longitudinal analysis of human wound environment. *J Invest Dermatol* 1994;103:660–664.
- Raju DR, Jindrak K, Weiner M, Enquist IF. A study of the critical bacterial inoculum to cause a stimulus to wound healing. *Surg Gynecol Obstet* 1977;144:347–350.
- Barrow RE, Meyer NA, Jeschke MG. Effect of varying burn sizes and ambient temperature on the hypermetabolic rate in thermally injured rats. *J Surg Res* 2001;99:253–257.
- Schaffer CJ, Reinisch L, Polis SL, Stricklin GP, Nanney LB. Comparison of wound healing among excisional, laser-created and standard thermal burns in porcine wounds of equal depth. *Wound Repair Regen* 1997;5:52–61.
- Miyajima S, Akaike T, Matsumoto K, Okamoto T, Yoshitake J, Hayashida K, Negi A, Maeda H. Matrix metalloproteinases induction by pseudomonas virulence factors and inflammatory cytokine *in vitro*. *Microb Pathogol* 2001;31:271–281.
- Wright JB, Lam K, Buret AG, Olson ME, Burrell RE. Early healing event in a porcine model of contaminated wounds: Effects of nanocrystalline silver on matrix metalloproteinases, cell apoptosis, and healing. *Wound Repair Regen* 2002;10:141–151.
- Boosalis MG, McCall JT, Ahrenholz DH, Solem LD, McClain CJ. Serum and urinary silver levels in thermal injury patients. *Surgery* 1987;101:40–43.
- Gear AJ, Hellewell TB, Wright HR, Mazzarese PM, Arnold PB, Rodeheaver GT, Edlich RF. A new silver sulfadiazine water soluble gel. *Burns* 1997;23:387–391.
- Babu R, Zhang J, Beckman EJ, Virji M, Pasculle WA, Wells A. Antimicrobial activities of silver used as a polymerization catalyst for a wound-healing matrix. *Biomaterials* 2006;27:4304–4314.